Journal of Engg. Research Vol. 9 No. (3A) September 2021 pp. 268-277 DOI : 10.36909/jer.v9i3A.7170

Crystallite Size on Micromechanical Characteristics of WO_3 Microparticles

Asep Bayu Dani Nandiyanto*, Farid Triawan**, Rubani Firly*** and Kikuo Kishimoto****

*Departemen Kimia, Universitas Pendidikan Indonesia, Jl. Dr. Setiabudi no 229, Bandung 40154, Indonesia
**Faculty of Engineering and Technology, Sampoerna University, Jl. Raya Pasar Minggu, Kav. 16, Pancoran, Jakarta, Indonesia
***Department of Mechanical Engineering, School of Engineering, Tokyo Institute of Technology, 2-12-1 Okayama, Meguro, Tokyo 152-8552, Japan
****Department of Transdisciplinary Science and Engineering, Tokyo Institute of Technology, 2-12-1 Ookayama, Meguro-ku, Tokyo 152-8552 Japan
*Corresponding Author: nandiyanto@upi.edu

Submitted: 08/08/2019
Revised: 16/01/2020
Accepted: 25/01/2020

ABSTRACT

This study evaluated the relationship between crystallite size and micromechanical characteristics of micrometer-sized monoclinic WO_3 particles. To avoid the existence of other parameters in the measurement (such as impurities and porous structure in the particle), micrometer WO_3 particles were prepared using a direct heat treatment of ultrapure micrometer-sized ammonium tungstate powders. The crystallite size was controlled independently in constant WO_3 particle outer diameters to obtain a precise measurement result. The mechanical properties, *i.e.*, hardness and Young's modulus, were measured by load-controlled nanoindentation test on the singular WO_3 particles. The force and displacement relationship data was plotted and analyzed to obtain the relationship between crystallite size and mechanical properties. The results revealed that the micromechanical properties of WO_3 particles were strongly dependent on the crystallite size. The hardness and Young's modulus values increased more than three times when increasing the crystallite size to about 40 nm. The study was completed with a proposed mechanism of crack propagation inside the particle due to static load. The study demonstrates the important role of crystallite size in determining the micromechanical characteristics of WO_3 particles. The result is useful especially when utilizing WO_3 microparticles for various processes involving extreme conditions, such as high pressure reaction.

Keywords: Tungsten trioxide; Micro-mechanical characteristics; Nanoindentation; Crystallite size; Hardness.

INTRODUCTION

One of the attractive factors in designing particles is crystallite size. Many reports have published information regarding the effect of crystallite sizes on material performance (Kumar and Münstedt, 2005; Nandiyanto *et al.*, 2020a; Nandiyanto *et al.*, 2020b). However, reports on the correlation between crystallite size and the mechanical performance of materials are still lacking, specifically in the case of micrometer-sized particles. In fact, this is important since it brings great impact to the sustainability properties of materials (Aloraier *et al.*, 2014; Mohamed *et al.*, 2014; Muhammad *et al.*, 2017; Şimşek and Uygunoğlu, 2018; Willems *et al.*, 1993).

Here, the purpose of this study was to evaluate the relationship between crystallite size and mechanical properties of micrometer-sized monoclinic tungsten trioxide (WO_3) particles. Micrometer-sized monoclinic WO_3 particles have attracted tremendous attention due to their excellent performance (*i.e.*, high mechanical strength, relatively harmlessness, active under visible light with good photo stability, chemical and thermal stability, and chemical and biological inertness), making them being applied in a variety of engineering uses. Although many reports showed the

way how to boost quality of WO_3-based materials (Arutanti *et al.*, 2014a; Arutanti *et al.*, 2014b; Nandiyanto *et al.*, 2013; Nandiyanto *et al.*, 2016; Nandiyanto *et al.*, 2019a; Nandiyanto *et al.*, 2020a; Nandiyanto *et al.*, 2020b), these materials still suffer from the information regarding mechanical properties. In fact, if there is no support from good understanding of their mechanical properties, the quality of designed WO_3 materials will be suboptimal. Thus, this information will be important to comprehend the best process condition when employing WO_3 materials. Until now, several papers have reported the mechanical properties of WO_3 (Abadias *et al.*, 2006; Hasan *et al.*, 2012; Maillé *et al.*, 2005; Parreira *et al.*, 2006). Most of the reports focused on the thin film, while reports on the WO_3 particles are disregarded. In fact, the material in particle form will be more applicable since it can be modified and reformed to larger and bulk materials.

To precisely uncover the impact of crystallite size on the mechanical properties, *i.e.*, hardness and Young's modulus, the present study used dense WO_3 particles, which were produced by direct heating ultrapure ammonium tungstate raw material (>99%) in the absence of additives and solvents. The existence of solvent and additive may trigger the change of particle morphology, as well as formation of porous structure inside the product (Nandiyanto *et al.*, 2013). Then, the crystallite size was controlled independently in constant WO_3 particle outer diameters to obtain a precise measurement result.

To evaluate mechanical properties of particles, different from common techniques that suffer from the need of complicated sample preparations (specifically additional process to compact the particles), the demand for relatively large quantity/size of sample and time-consuming procedures, and the ignorance of influences of porosity, particle size and shape, and changing potential mechanical properties (during the compaction process) (Masterson and Cao, 2008; Taylor *et al.*, 2004), we used the nanoindentation technique that allows indentation measurements directly to the sample (e.g., thin films, individual particles, or crystals (Fischer-Cripps, 2006; Inoue *et al.*, 2019; Li and Bhushan, 2002; Masterson and Cao, 2008; Olivas *et al.*, 2006; Taylor *et al.*, 2004)). To reveal the relationship between crystallite size and mechanical properties, the results of nanoindentation test were plotted and analyzed. The results were also completed with an explanation and proposed mechanism of crack propagation inside the particle due to static load based on current finding. This is important issue since it can decide mechanical properties (Nurprasetio et al., 2017 &).

In addition, there are two categories of tests in evaluating mechanical properties: macro- (load greater than 1 kg) and micromechanical (load less than 1 kg) (Willems *et al.*, 1993). In this study, we focused on the micromechanical properties of WO_3, specifically Young's modulus (E) and hardness (H). E reflects the resistance of a material to the elastic deformation, whereas H reflects the resistance of a material to the plastic deformation (Taylor *et al.*, 2004). We believe that the values of E and H can reflect the mechanical characteristics of micrometer-sized WO_3 particles.

METHOD

As a specimen, WO_3 microparticles were used in this study with various crystallite sizes. WO_3 particles themselves were prepared using the method described in detail in our previous works (Nandiyanto *et al.*, 2016; Nandiyanto *et al.*, 2020a; Nandiyanto *et al.*, 2020b). Briefly, the WO_3 particles were produced by direct heating of ammonium tungstate pentahydrate (ATP; >99%; Kanto Chemical Co., Inc., Japan). To control the crystallite size, the heating process was set at a specific temperature ranging between 240 and 800°C. Then, to confirm the successful preparation of WO_3 particles in the specific crystal size, the prepared particles were then evaluated using the following characterizations: (1) analysis of particle size and morphology: Scanning Electron Microscope (SEM; SEM, JSM-6360LA; JEOL Ltd., Japan) and a Transmission Electron Microscope (TEM, JEOL JEM-1400, JEOL Ltd., Japan); and (2) analysis of chemical composition and crystal structure: a Fourier Transform Infrared Spectroscopy (FTIR; FTIR-4600, Jasco Corp., Japan) and a powder X-ray diffraction (XRD; XRD; PANalytical X'Pert PRO; Philips Corp., The Netherland).

For the evaluation of micromechanical characteristics (*i.e.*, hardness (*H)* and Young's modulus (*E*)) of the samples, the WO_3 specimen was diluted into methanol, spread out into the specimen holder, and put into the nanoindentation test technique apparatus (TriboScope®, Hysitron, US) equipped with portable add-on equipment to scanning probe microscope (SPM, SPM-9500J3, Shimadzu Corp., Japan). To confirm the precise nanoindentation measurements, all data were compared with the aluminum bulk plate standard. Each measurement was conducted more than five times at different locations in the sample. The analysis results were then plotted to get the loading force and displacement data curves. The curves were normalized with the mechanical properties of ATP (sample before heat treatment). Detailed information for the nanoindentation test is explained in previous literature (Nandiyanto *et al.*, 2019a).

RESULTS AND DISCUSSION

The SEM images, presented in Figs. 1a and b, respectively, show the particles before and after heat treatment (800°C). The change in the particle sizes after heat treatment has been found. But, all particle sizes are in the micrometer range. This phenomenon is in a good agreement with previous studies (Nandiyanto *et al.*, 2016; Nandiyanto *et al.*, 2020a), which is due to the existence of released gas during the decomposition of ATP into WO_3.

The high-magnified SEM images (Figs. 1c, d, and e) showed that the particles have cubical shapes with different surface roughness. The increases in the heating temperatures resulted in the formation of rougher surface (as shown in Fig. 1e), replying to the existence of enlarging crystallite sizes.

XRD analysis results of the particles prepared with various heating temperatures were presented in Fig. 1f. The measurement was focused on between 20 and 40°C, which was used for confirming the crystal structure and measuring the Scherer crystallite size (*Dc*). Detailed information for the XRD analysis has been explained in our previous works (Nandiyanto *et al.*, 2020a; Nandiyanto *et al.*, 2020b). It is revealed that the amorphous was started from 240°C, whereas fully crystalline material was from 320°C. Then, the increasing temperature had impact to increase the crystallite sizes up.

To confirm the analysis, FTIR was done. All FTIR results were compared to the standard FTIR spectra (Nandiyanto *et al.*, 2019b). The results showed that there is a change in the FTIR patterns, confirming the XRD results in Fig. 1f.

To confirm the structure inside the particle, TEM analysis was conducted (Figs. 1g and h). We analyzed samples heated at 240 (Fig. 1g) and 800°C (Fig. 1h), which were sufficient to represent the WO_3 with amorphous and crystal phases, respectively. TEM images confirmed that all materials were dense, and the existence of crystallites was detected (see the red area in Fig. 1e). The sizes of the crystallites in Fig. 1h were in a good relationship with the observation of surface roughness in SEM image in Fig. 1e and the measurement of XRD Scherer crystal size in Fig. 1f. The increases in the temperature lead to enlarging crystallite size without giving impact on changing the porosity in the particle since the present preparation process used an additive-free process.

Fig. 1i is the AFM image of sample after nanoindentation. For verification purposes, we also conducted nanoindentation test on aluminum bulk material (Fig. 1j). The images showed the indented part after the load was released. A crack formation can be seen on the particle (see the red arrow in Fig. 1i), which is different from common nanoindentation test (see the red arrow in Fig. 1j).

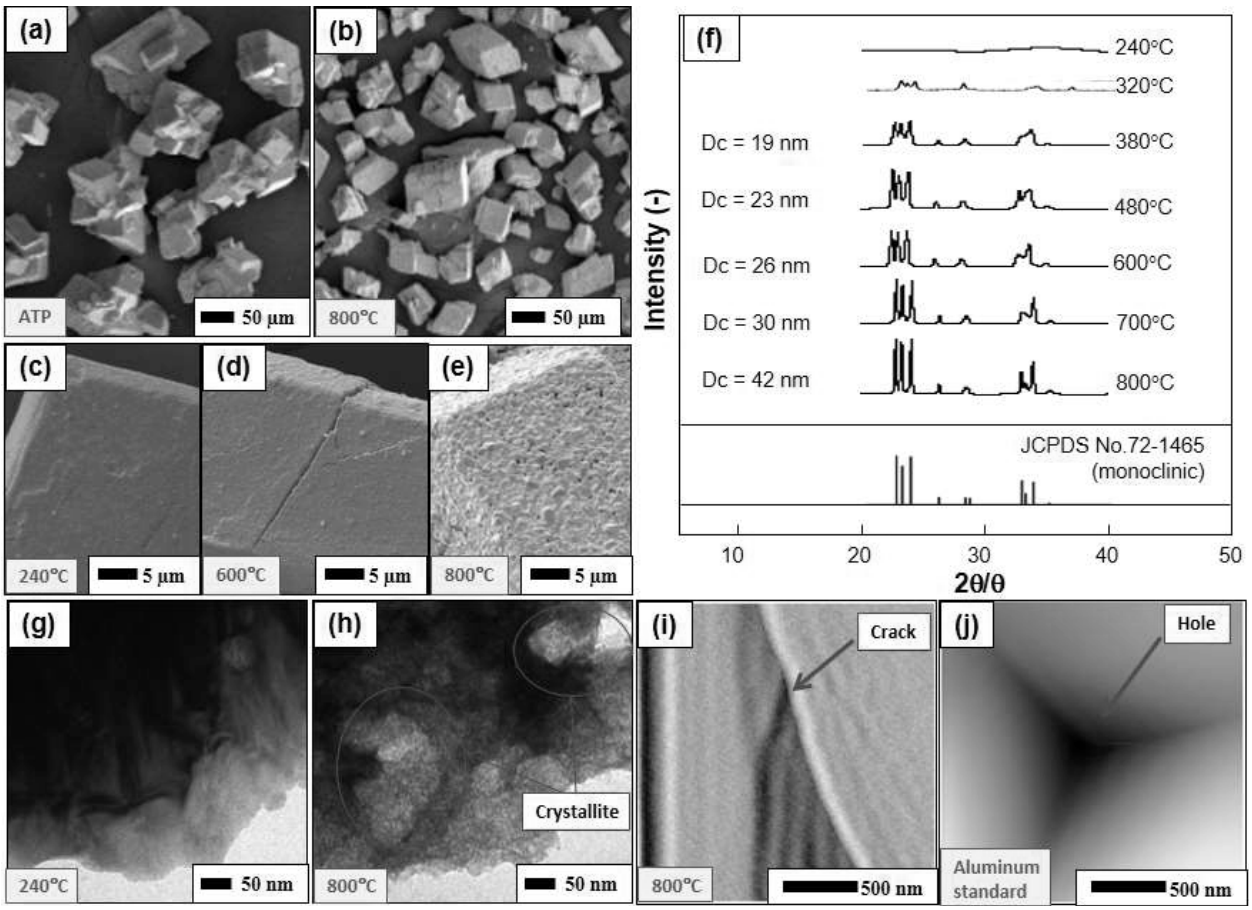

Figure 1. The SEM (a-e), XRD (f), TEM (g,h), and AFM (i,j) images of samples. (a) and (b) are the low-magnified SEM images of ATP and WO_3 prepared by heating ATP at 800°C, respectively. (c), (d), and (e) are the high-magnified SEM images of WO_3 prepared by heating at 240, 600, and 800°C, respectively. (g) and (h) are the high-magnified TEM images of WO_3 prepared by heating at 240 and 800°C, respectively. (i) and (j) are the AFM images of samples after nanoindentation process for samples of WO_3 prepared by heating ATP at 800°C and aluminum standard, respectively. *Dc* is the Scherer crystallite size.

To evaluate the effect of crystallite size on the micromechanical properties of WO_3 particles, we plotted the relationship of particle outer diameter (*Dp*), crystallite size (*Dc*), and mechanical properties of WO_3 particles (*i.e.*, *H* and *E*) under various heating temperatures of the WO_3 preparation process (see Fig. 2). Each measurement was done more than five times to ensure and guarantee the repeatability of the experiments. The curve was also completed with standard deviation for each data.

Based on our previous reports (Nandiyanto *et al.*, 2020a), the figure was divided into three zones: (1) less than 240°C (ammonium tungstate zone); (2) between 240 and 320°C (amorphous zone); and (3) more than 320°C (crystalline zone).

In the first zone (ammonium tungstate zone), there is no change in the chemical structure of ammonium tungstate. *Dp* decreased with increasing temperature, which was due to the release of water molecules from the ATP particle (Nandiyanto *et al.*, 2016; Nandiyanto *et al.*, 2020a). Since this temperature has no WO_3 structure, we did not focus on it, and we tended to neglect this zone for the further analysis of micromechanical properties.

In the second zone (amorphous zone), increasing temperature corresponds to the crystalline content in the particle (transformation of amorphous into crystalline) (Nandiyanto *et al.*, 2020b). Major changes in the *Dp* were obtained. Better values of *H* and *E* in this zone were obtained compared to those in the first zone. However, changing the crystalline content has no impact on the values of *H* and *E*.

In the third zone (crystalline zone), increasing temperature no more has impact on the *Dp*. This constant *Dp* is because there is no change in the chemical content in the particle (Nandiyanto *et al.*, 2020a). The change in *Dc* was obtained. Since *Dp* is constant, the relationship between *Dc* and micromechanical characteristics of WO_3 can be investigated precisely. We found the obtainment of high mechanical strength material, in which the *H* and *E* values increase more than three times when heating at 800°C (*Dc* of about 40 nm). The present trend for the effect of heating temperature on the mechanical properties is in good agreement with previous studies (Hasan *et al.*, 2012). Based on the above analysis, it is found that *Dc* has a more significant impact on the change of micromechanical structure.

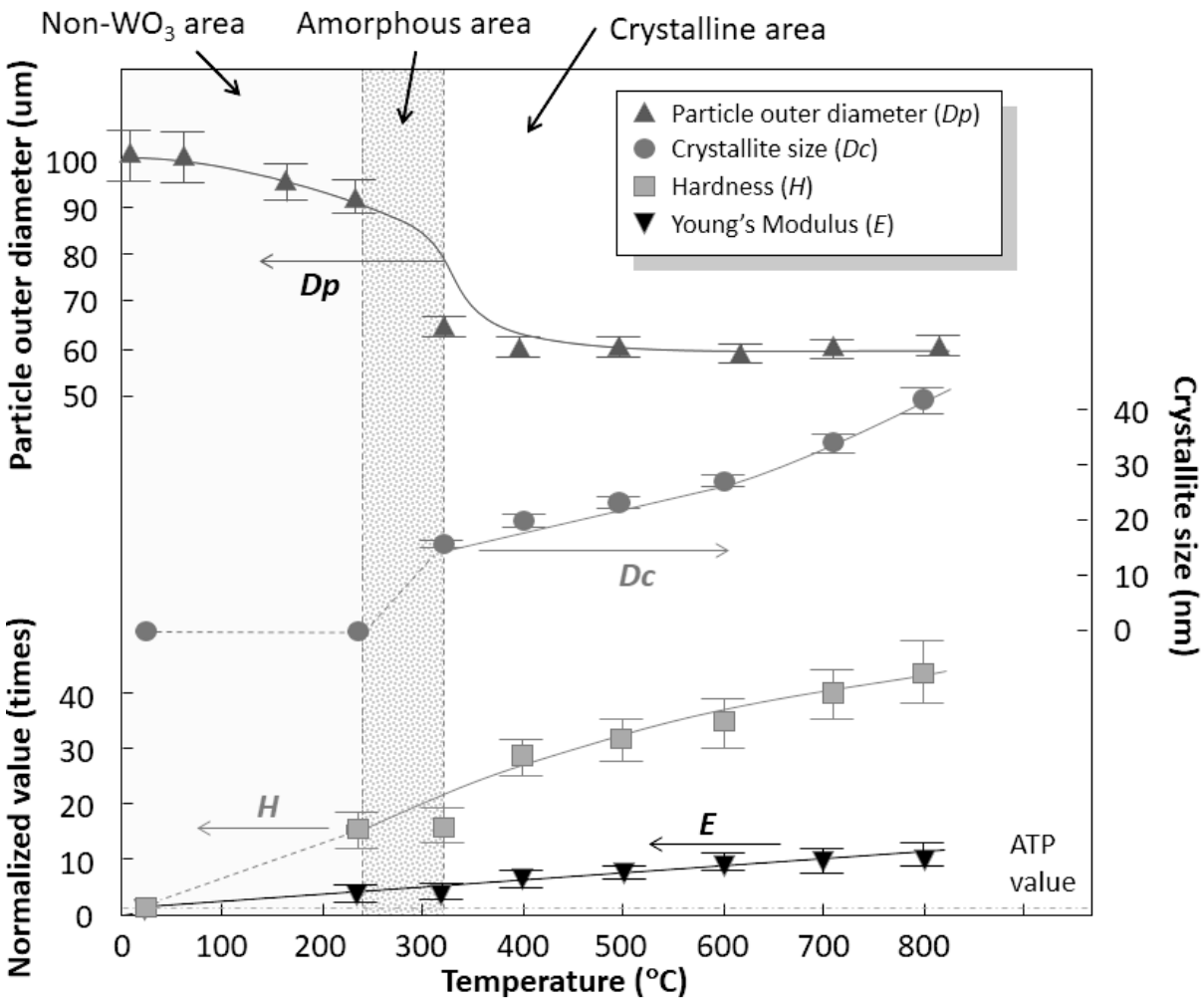

Figure 2. Plotted curves of particle outer diameter, crystallite size, hardness, and increasing values of micromechanical properties as a function of heating temperature. Blue dashed and dotted line () is the standard ATP value.

To confirm the analysis in Figure 2, Figure 3 shows the normalized values of micromechanical properties of WO_3 particles versus crystallite size. From the above results, the strong influences of crystallite size on the mechanical properties of WO_3 particles in terms of both *H* and *E* were observed.

Taking the amorphous sample (see the red area in Figure 3), we found that there is a jump in the mechanical properties values compared to the ATP. The values of *H* and *E* improved to more than three times. This implies that the microstructure of WO_3 enhances the mechanical properties. ATP itself suffered from the condition of very sensitive to cracks. It might be due to the existence of organic structure (such as ammonium and water molecules) inside its body (see the dashed area in Figure 3).

When adding higher temperature of heating process (up to 320°C) to the sample, the crystal structure begins to be formed. As explained in the literature (Nandiyanto *et al.*, 2020b), the increases in temperature from 240 to 320°C lead to the conversion of amorphous into crystalline. By increasing the temperature, the amorphous content decreases, while the number of crystalline structures increases. However, the increasing level of crystallinity in the particle did not improve much the mechanical properties of material, implying the strong influences of amorphous content on the mechanical structure of material.

Further increases in the temperature (more than 320°C), which promote the enlarging crystallite (Nandiyanto *et al.*, 2020a), bring positive effects on the mechanical properties. The values of *H* and *E* increased from 14 to 43 times and from 3 to 9 times, respectively, as the increases in the crystallite sizes indicate the significant impact of the crystallite size on the mechanical properties of material (Boyd, 1985).

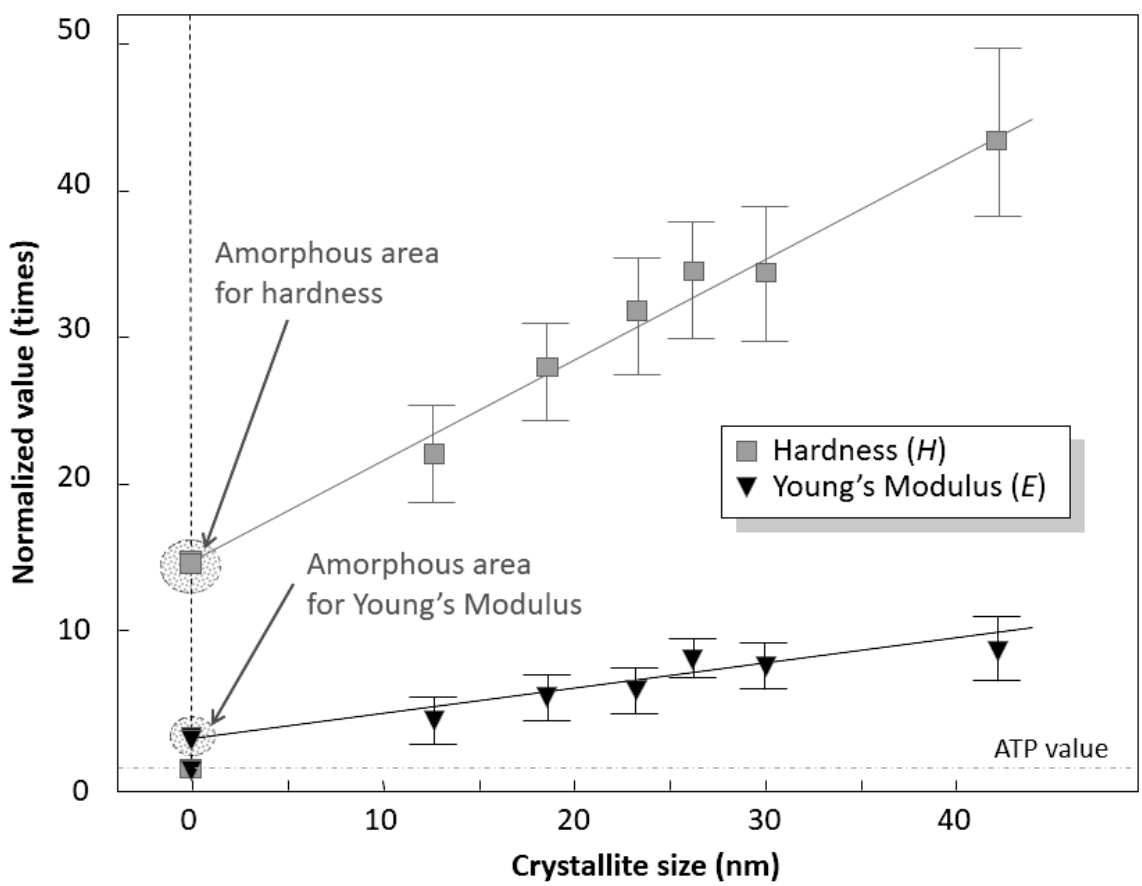

Figure 3. Comparison hardness and Young's modulus under various crystallite sizes. Blue dashed and dotted line is the standard ATP value

To clearly understand the above phenomena in Figures 2 and 3, hypothesis on the crack propagation mechanism inside the particle is presented in Table 1. This table shows a 2-dimensional illustration model of crack propagation path during the nanoindentation test. The actual mark of crack on the particle can be seen in Fig. 1i, which has a different shape with the common nanoindentation test mark on an aluminum bulk material (Fig. 1j).

Table 1. 2-dimensional illustration model of particle crack during mechanical testing. Blue area and orange area are the areas of amorphous component and crystallite, respectively. Red arrow ( ) is the position of crack pressure by nanoindentation tip, and red line is the crack path in the material. Blue cross is the position of cross stop.

Type	Model	Crack Model
Amorphous		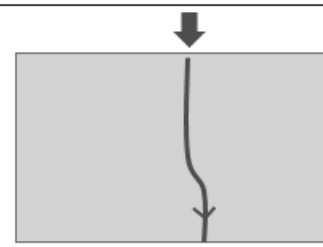
Amorphous (with some crystalline content)	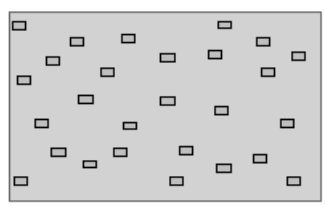	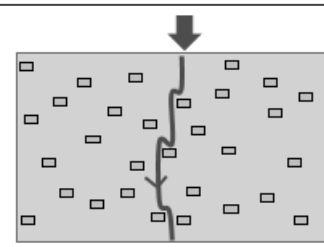
Crystalline (with small crystallites)	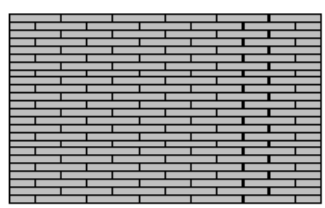	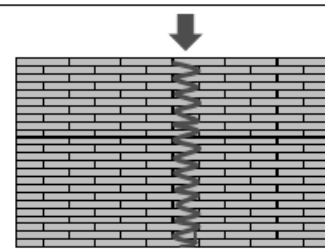
Crystalline (with larger crystallites)	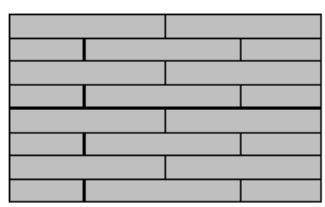	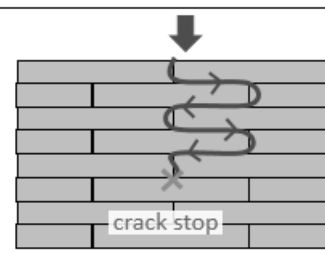

Amorphous does not possess long periodicity of atoms (see the blue area in Table 1) compared to crystalline (see the orange area in Table 1). Amorphous has only few atomic orders in the level of molecular dimensions (very short range). Atoms in the amorphous are distributed randomly in 3-dimensional space. This is different with crystalline that has very long range of atomic order. Atoms in crystalline are strong. Atoms inside the crystallite have more time

to perform thermal fluctuations, making them possible to overcome the physical energy that can cause the bonds to break (Lei *et al.*, 2018).

When there is a load pressure on the material (see the red arrow in Table 1), the crack will propagate to a region with less energy bonding in the atomic structure. Since the amorphous has distributed atomic arrangement in the material, applying physical force on amorphous material results in direct crack of material. The crack in the amorphous material can happen in all positions.

When the amorphous material is mixed with some crystalline structure, the applied load pressure allows the formation of crack and then propagates in the area in between the crystallites. The nanoindentation tip breaks the atomic bonding that is in the amorphous phase, while the crystallites themselves still remained (no change) (Lee *et al.*, 2005). A similar mechanism of crack propagation in composite materials is also explained by other reports (Budiman et al., 2017; Budiman et al., 2018; Triawan et al., 2020). These hypotheses also explained the main reason for the similar mechanical properties of amorphous material with various crystalline amounts.

Regarding the fully crystalline material, we measured high values of H and E. Atoms are in good arrangement inside the crystallite. This condition makes the atomic bonding difficult to be broken. When applying the load pressure, the interface between crystallites (as a layer between crystallites) plays important roles in the behavior of crack propagation mechanism (Budiman *et al.*, 2018; Sangid *et al.*, 2011; Zhai *et al.*, 2000). The formed cracks have to find paths with the lowest interfacial energy to propagate inside the particle. When the material has small crystallites, crack can find propagation paths easily (since small crystallites have large area of interface). However, when the material has large crystallites, the crack must go longer paths to propagate (compared to the paths in the material with small crystallites), or even it could be stopped by the crystallite itself. This makes the particle require higher energy to deform and break. It means that a particle with large crystallites can overcome large load and maintain its structure (Liu *et al.*, 2013). In other words, the particles become much stronger with larger crystallites.

The crack phenomena have a complicated mechanism. Many parameters influence the condition of crack, such as surface roughness, wettability, chemical bonding reaction, and electrostatic bonding (Budiman *et al.*, 2017; Budiman *et al.*, 2018), in which these will be discussed in our future work. In addition, although the present technique is effective to distinguish and quantify the mechanical properties, other results should be considered because the standard deviation is quite high, in which some data are near to 27%. This indicates the potentially error in the position of nanoindentation tip on the particle during the measurement.

CONCLUSION

The relationship between crystallite size and the mechanical properties of micrometer-sized monoclinic WO_3 particles has been studied. It is found that the crystallite size plays an important role in improving mechanical properties, *i.e.*, hardness and Young's modulus, of the WO_3 particles. The hardness and Young's modulus values increase more than three times, when increasing the crystallite sizes to about 40 nm. The present results bring information for further studies in the mechanical properties of WO_3 material. Moreover, it was also revealed that the WO_3 micron particles have significantly higher values of hardness and elastic modulus compared with those of ATP particles. We believe that this data can inform that micrometer-sized WO_3 particles are potentially used for various processes involving extreme conditions, such as high pressure reaction.

ACKNOWLEDGMENT

RISTEK DIKTI (grant-in-aid Penelitian Terapan Unggulan Perguruan Tinggi (PTUPT)) is acknowledged.

REFERENCES

Abadias, G., Dub, S. & Shmegera, R. 2006. Nanoindentation hardness and structure of ion beam sputtered TiN, W and TiN/W multilayer hard coatings. Surface and coatings technology, **200**(22-23): 6538-6543.

Aloraier, A., Al-Fadhalah, K., Paradowska, A.M. & Alfaraj, E. 2014. Effect of welding polarity on bead geometry, microstructure, microhardness, and residual stresses of 1020 steel. Journal of Engineering Research, 4(2): 1-24.

Arutanti, O., Nandiyanto, A.B.D., Ogi, T., Iskandar, F., Kim, T.O. & Okuyama, K. 2014a. Synthesis of composite WO3/TiO2 nanoparticles by flame-assisted spray pyrolysis and their photocatalytic activity. Journal of alloys and compounds, **591**: 121-126.

Arutanti, O., Ogi, T., Nandiyanto, A.B.D., Iskandar, F. & Okuyama, K. 2014b. Controllable crystallite and particle sizes of WO3 particles prepared by a spray-pyrolysis method and their photocatalytic activity. AIChE Journal, **60**(1): 41-49.

Bale, J.S., Pell, Y.M., Jafri, M., & Selan, R. 2019. Experimental investigation on mechanical joint of lontar (borassus flabellifer) fiber reinforced polyester composites under static flexural test. Indonesian Journal of Science and Technology, **4**(1): 17-27.

Boyd, R.H. 1985. Relaxation processes in crystalline polymers: experimental behaviour—a review. Polymer, **26**(3): 323-347.

Budiman, B.A., Triawan, F., Adziman, F. & Nurprasetio, I.P. 2017. Modeling of stress transfer behavior in fiber-matrix composite under axial and transverse loadings. Composite Interfaces, **24**(7): 677-690.

Budiman, B.A., Adziman, F., Sambegoro, P.L., Nurprasetio, I.P., Ilhamsyah, R. & Aziz, M. 2018. The role of interfacial rigidity to crack propagation path in fiber reinforced polymer composite. Fibers and Polymers, **19**(9): 1980-1988.

Fischer-Cripps, A.C. 2006. Critical review of analysis and interpretation of nanoindentation test data. Surface and coatings technology, **200**(14-15): 4153-4165.

Hasan, M., Haseeb, A. & Masjuki, H. 2012. Structural and mechanical properties of nanostructured tungsten oxide thin films. Surface Engineering, **28**(10): 778-785.

Inoue, K., Triawan, F., Inaba, K., Kishimoto, K., Nishi, M., Sekiya, M., Sekido, K. & Saitoh, A. 2019. Evaluation of interfacial strength of multilayer thin films polymer by nanoindentation technique. Mechanical Engineering Journal, **6**(1): 18-00326-18-00326.

Kumar, R. & Münstedt, H. 2005. Polyamide/silver antimicrobials: effect of crystallinity on the silver ion release. Polymer International, **54**(8): 1180-1186.

Lee, J.G., Lee, D.G., Lee, S., Cho, K.m., Park, I. & Kim, N.J. 2005. Effects of crystalline particles on mechanical properties of strip-cast Zr-base bulk amorphous alloy. Materials Science and Engineering: **A 390**(1-2): 427-436.

Lei, S., Cao, Q., Geng, X., Yang, Y., Liu, S. & Peng, Q. 2018. The Mechanical Properties of Defective Graphyne. Crystals, **8**(12): 465.

Li, X. & Bhushan, B. 2002. A review of nanoindentation continuous stiffness measurement technique and its applications. Materials characterization, **48**(1): 11-36.

Liu, X., Yuan, F. & Wei, Y. 2013. Grain size effect on the hardness of nanocrystal measured by the nanosize indenter. Applied Surface Science, **279**: 159-166.

Maillé, L., Sant, C., Aubert, P. & Garnier, P. 2005. Morphological and mechanical properties study of [WO3/W] n nanoscale multilayers. Thin Solid Films, **479**(1-2): 201-206.

Masterson, V.M. & Cao, X. 2008. Evaluating particle hardness of pharmaceutical solids using AFM nanoindentation. International Journal of Pharmaceutics, **362**(1-2): 163-171.

Mohamed, A., Alkhaledi, K. & Cochran, D. 2014. Estimation of mechanical properties of soft tissue subjected to dynamic impact. Journal of Engineering Research, **4**(2): 1-15.

Muhammad, M., Siddiqui, M.A. & Muhammad, S. 2017. Experimental investigation and optimization of process parameters for through induction hardening using factorial design of experiments. Journal of Engineering Research, **5**(3): 174-185.

Nandiyanto, A.B.D., Arutanti, O., Ogi, T., Iskandar, F., Kim, T.O. & Okuyama, K. 2013. Synthesis of spherical macroporous WO3 particles and their high photocatalytic performance. Chemical engineering science, **101**: 523-532.

Nandiyanto, A.B.D., Munawaroh, H.S.H., Kurniawan, T. & Mudzakir, A. 2016. Influences of temperature on the conversion of ammonium tungstate pentahydrate to tungsten oxide particles with controllable sizes, crystallinities, and physical properties. Indonesian journal of chemistry, **16**(2): 124-129.

Nandiyanto, A.B.D., Zaen, R. & Oktiani, R. 2020. Correlation between crystallite size and photocatalytic performance of

micrometer-sized monoclinic WO3 particles. Arabian Journal of Chemistry, **13**(1): 1283-1296.

Nandiyanto, A.B.D., Oktiani, R., Ragadhita, R., Sukmafitri, A. & Zaen, R. 2020. Amorphous content on the photocatalytic performance of micrometer-sized tungsten trioxide particles. Arabian Journal of Chemistry 13(1): 2912-2924.

Nandiyanto, A.B.D., Triawan, F., Firly, R., Abdullah, A.G., Aono, Y., Inaba, K. & Kishimoto, K. 2019a. Identification of micro-mechanical characteristics of monoclinic tungsten trioxide microparticles by nanoindentation technique. Materials Physics and Mechanics, **42**(3): 323-329.

Nandiyanto, A.B.D., Oktiani, R., & Ragadhita, R. 2019b. How to Read and Interpret FTIR Spectroscope of Organic Material. Indonesian Journal of Science and Technology, **4**(1): 97-118.

Nurprasetio, I.P., Budiman, B.A., & Triawan, F. 2017. Failure investigation of plastic shredding machine's flange coupling based on mechanical analysis. Indonesian Journal of Science and Technology, **2**(2): 124-133.

Olivas, E., Swadener, J. & Shen, Y.L. 2006. Nanoindentation measurement of surface residual stresses in particle-reinforced metal matrix composites. Scripta Materialia, **54**(2): 263-268.

Parreira, N., Carvalho, N. & Cavaleiro, A. 2006. Synthesis, structural and mechanical characterization of sputtered tungsten oxide coatings. Thin Solid Films, **510**(1-2): 191-196.

Sangid, M.D., Maier, H.J. & Sehitoglu, H. 2011. The role of grain boundaries on fatigue crack initiation–an energy approach. International Journal of Plasticity, **27**(5): 801-821.

Şimşek, B. & Uygunoğlu, T. 2018. A design of experiment application to improve raw materials utilization ratio of polymer concrete composites. Journal of Engineering Research, **5**(4): 1-18.

Taylor, L., Papadopoulos, D., Dunn, P., Bentham, A., Mitchell, J. & Snowden, M. 2004. Mechanical characterisation of powders using nanoindentation. Powder Technology, **143**: 179-185.

Triawan, F., Nandiyanto, A.B.D., Suryani, I.O., Fiandini, M., & Budiman, B.A. 2020. The influence of turmeric microparticles amount on the mechanical and biodegradation properties of cornstarch-based bioplastic material: From bioplastic literature review to experiments. Materials Physics and Mechanics, **46**(1): 99-114.

Willems, G., Celis, J.P., Lambrechts, P., Braem, M. & Vanherle, G. 1993. Hardness and Young's modulus determined by nanoindentation technique of filler particles of dental restorative materials compared with human enamel. Journal of biomedical materials research, **27**(6): 747-755.

Zhai, T.g., Wilkinson, A. & Martin, J. 2000. A crystallographic mechanism for fatigue crack propagation through grain boundaries. Acta Materialia, **48**(20): 4917-4927.